

Formation of Long-Range-Ordered Nanocrystal Superlattices on Silicon Nitride Substrates

X. M. Lin,^{*,†} H. M. Jaeger,[‡] C. M. Sorensen,[‡] and K. J. Klabunde[‡]

*The James Franck Institute, The University of Chicago, 5640 South Ellis Avenue, Chicago, Illinois 60637, and
Department of Physics and Chemistry, Kansas State University, Manhattan, Kansas 66506*

Received: January 18, 2001

Particle–particle and particle–substrate interactions cause nanocrystals to self-assemble into superlattice structures upon drying from a colloidal suspension on a solid surface. Rapid dewetting of a volatile solvent, however, can significantly undermine the degree of ordering. We demonstrate here that by increasing the concentration of the nonvolatile dodecanethiol ligand, dewetting can be controlled and gold nanocrystal superlattices can be formed on silicon nitride substrates with long range ordering over several microns. Monolayer and bilayer superlattices can be produced by adjusting the nanocrystal concentration. The superlattice structures are robust and are not perturbed by the final dewetting of the solvent.

I. Introduction

Periodicity is one of nature's fundamental beauties.¹ Ordering on the atomic scale produces energy bands that determine the electrical and optical properties of crystalline materials.² On the other hand, the lack of symmetry can lead to distinctly different properties that are unique to noncrystalline materials.³ Recent synthetic developments in the fabrication of highly monodispersed nanocrystals allow us to study the role of periodicity on a different length scale, using building blocks with sizes on the order of nanometers.^{4–6} Superlattices made from these building blocks give us the opportunity to study not only the properties of the individual building blocks, but also collective electronic effects such as the metal–insulator transition⁷ and magnetism.⁸ In a colloidal suspension, individual nanocrystals may be viewed as analogous to dissolved molecules. As the solvent evaporates from a droplet of such a colloid on a substrate, the solubility limit will be exceeded and a superlattice of nanocrystals can nucleate on the surface because of both particle–particle and particle–substrate interactions. So far, metal, metal oxide, and semiconductor nanocrystals have been shown to self-assemble into ordered structures upon evaporation of the solvent on a solid substrate or on a water–air interface.^{9–17} However, the resulting morphologies and the degree of the ordering achieved vary significantly. Most of the nanocrystal superlattices reported so far have ordered domain sizes less than a few hundred nanometers. Spatial disorder can induce undesirable change to the electronic and optical properties of the nanocrystal network.¹⁸ Experimentally, periodicity with long-range ordering is hard to achieve not only because of the intrinsic particle size distribution but also because of the dewetting of the solvent during the self-assembly process. Korgel and Fitzmaurice suggested that the polarity of the solvent affects its wetting properties and subsequently influences the aggregation of nanocrystals on the surface.¹⁹ Ohara et al. and Gelbart et al. examined the mechanism of solvent dewetting in annular ring structures formed by drying a diluted metal colloid on a solid substrate.^{20,21}

In this letter, we will show that the morphology of the domain structures in gold nanocrystal arrays is determined by a competition between two-dimensional superlattice formation and

solvent dewetting. We demonstrate that, by controlling the dewetting process of the solvent, long-range-ordered nanocrystal superlattices can be prepared routinely, with domains size of several microns.

II. Nanocrystal Synthesis

Gold nanocrystals were synthesized according to a procedure previously developed by some of us.²² Unlike the widely used two phase synthesis that was pioneered by Brust et al.,⁵ our synthesis is a single-phase reaction in a cationic surfactant solution. The as-prepared nanocrystals were then coated with dodecanethiol through ligand exchange. We have also shown that, by adopting a digestive ripening process in an environment of excess thiol, the particle size distribution can be greatly narrowed. Further size segregation by lowering the colloid temperature can produce highly monodispersed nanocrystals of 5.5 nm diameter (relative standard deviation ~5%).

A typical synthesis proceeds as follows. HPLC grade toluene (Fisher) is first distilled with potassium and sodium metals. Distilled toluene is then bubbled with dry argon gas for 2 h. A total of 51 mg of gold chloride (99.99%, Aldrich) is dissolved by sonication in a 15 mL of 0.025 M didodecyltrimethylammonium bromide (Fluka) toluene solution. A total of 54 μ L of 9.4 M NaBH₄ aqueous solution is added dropwise to the reaction flask while stirring the solution at room temperature. A red-colored gold colloid forms after 15 min. A total of 0.2 mL of dodecanethiol is added to the 2.5 mL of gold colloid to ligate the gold surface through ligand exchange. Gold nanocrystals are then precipitated with ethanol, vacuum-dried and, redissolved into 2.5 mL of toluene. Another 0.2 mL of dodecanethiol is added, and the colloid is heated under reflux for more than 10 min. It was found that the size distribution of nanocrystals can be significantly narrowed when refluxed with dodecanethiol ligand. The heated colloid is then diluted by adding heated toluene to 7.5 mL. The vial is left on the benchtop for more than 1 day, and further size segregation occurs during the slow lowering of the colloid temperature. As a result, the top layer of the gold colloid becomes highly monodisperse. The top layer is separated, vacuum-dried, and washed with ethanol repeatedly to remove excess thiol. The precipitates are finally dissolved in pure toluene to form a colloid of the desired nanocrystal concentration.

* To whom correspondence should be addressed.

[†] The University of Chicago.

[‡] Kansas State University.

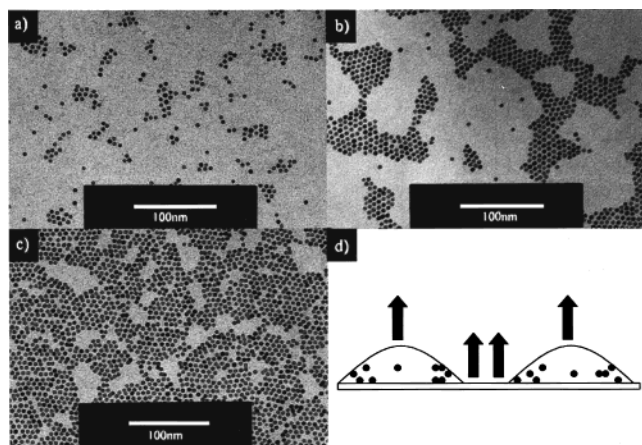


Figure 1. Nanocrystal patterns formed by depositing 10 μL of gold nanocrystal colloid in pure toluene on 3 mm \times 4 mm silicon nitride substrates with various particle concentration (a) 1.0×10^{12} , (b) 4.8×10^{12} , and (c) $1.2 \times 10^{13} \text{ mL}^{-1}$. The schematic diagram in (d) illustrates the formation of domain structures in a dewetting film.

III. Self-Assembly

As substrates, we used silicon wafers with a 100 nm thick amorphous silicon nitride layer. The wafers were etched from

the backside to open a window area (60–200 μm), consisting of a free-standing silicon nitride membrane.²³ This allowed characterization by transmission electron microscope (TEM) and atomic force microscopy (AFM) without removing the sample from the substrate. AFM on the bare substrate showed a surface roughness of 1–2 nm. Our substrates had lateral dimensions of 3 mm \times 4 mm, with a window in the middle. All substrates were cleaned with toluene, acetone, methanol, and distilled water on a spinner prior to the experiment and dried with high purity nitrogen gas.

A range of different monolayer patterns were observed when we evaporated the gold colloid using pure toluene as the solvent (the residue thiol volume fraction in these colloids was less than 5×10^{-4}). With pure toluene solvent, the liquid film may thin enough before the nucleation limit is reached so that dewetting from the substrate occurs before superlattice formation. A typical set of patterns is shown in Figure 1. When we increased the particle concentration, the pattern morphology changed from small isolated domain structures to percolating domains and eventually to compact domains. These different structures are frequently seen in the literature as well.^{15–17,19} Dewetting causes holes to open up in the liquid layer and particles to move outward, away from the holes, as the liquid evaporates. On the other hand, convective flow inside wetting droplets has the

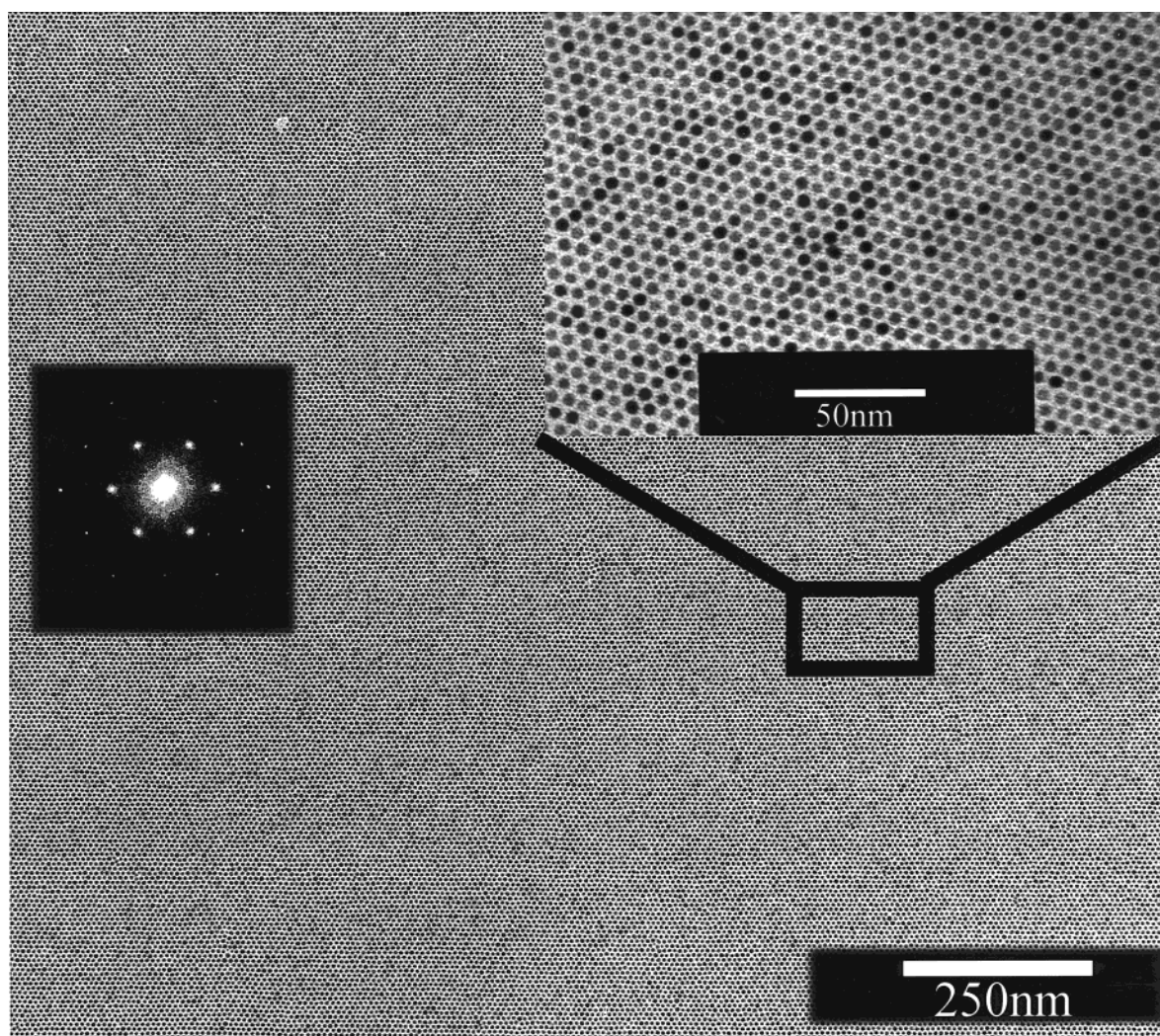


Figure 2. Long-range-ordered nanocrystal monolayer formed by 10 μL of colloid in the toluene dodecanethiol mixture, with a thiol volume fraction of 6.3×10^{-3} and particle concentration of $1.2 \times 10^{13} \text{ mL}^{-1}$. Only a quarter of this single-crystal monolayer is shown here in order to demonstrate the ordering while keeping the individual nanocrystals visible. The upper right inset shows a detailed view. The left inset shows the diffraction pattern obtained by Fourier transformation of a portion of the TEM negative.

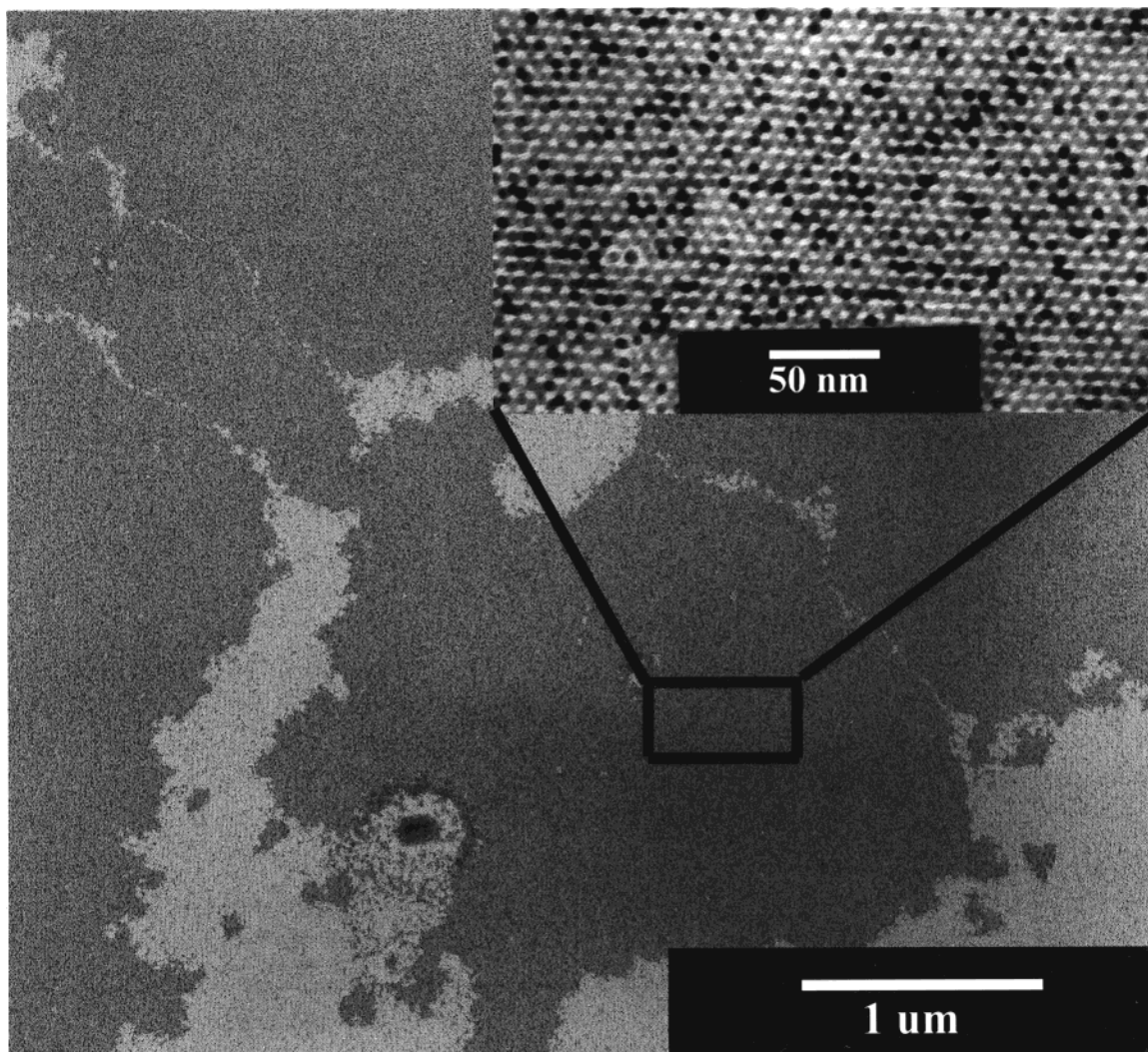


Figure 3. Highly ordered nanocrystal bilayer formed by 10 μL of colloid in the toluene dodecanethiol mixture, with a thiol volume fraction of 6.3×10^{-3} and particle concentration of $2.4 \times 10^{13} \text{ mL}^{-1}$. The brighter areas in the figure contain a highly ordered monolayer similar to the one in Figure 2. The darker patches are extended bilayer regions. The inset shows an enlarged portion of the bilayer.

tendency to drive the particles in the opposite direction.²⁴ Only when the interactions between particles and the substrate and between particles are strong enough will the nanocrystals be pinned to the substrate. The domains thus formed depend on the nanocrystal concentration. Isolated domains of nanocrystals form at low particle concentration when the pinning effect is weak and dewetting holes percolate across the substrate (Figure 1a). As the particle concentration increases, the pinning effect becomes stronger because of the increase frequency of particle–particle interactions. Dewetting holes then become more isolated and percolating particle domains form (Figure 1b). At an even higher particle concentration, the sizes of the dewetting holes decrease significantly and a more compact monolayer is formed (Figure 1c). In addition to the effect of dewetting, a recent AFM study²⁵ has shown that the interparticle interaction might become strong enough to cause spinodal phase separation during the liquid drying process. This effect would also cause particles to form percolating domains. Despite the strong pinning effect and the entropy-driven ordering tendency in the case of high particle concentrations, local disorder and voids are still inevitable in a compacted monolayer. We found that further increasing the particle concentration does not improve the monolayer ordering significantly before bilayer formation starts to appear.

To maintain a wetting layer on the surface so that nanocrystals can have a chance to self-assemble into large periodical

structures, the evaporation rate of the solvent must be slowed. In analogy to molecular crystallization, it is reasonable to propose that better superlattices, larger and with fewer defects, are obtained when they form slowly. Once formed, these superlattices may be tough enough not to be perturbed when dewetting finally occurs. Widmann et al. found that adding a nonvolatile additive to liquid aerosol droplets can significantly slow their evaporation rate.²⁶ In our case, excess low-volatile dodecanethiol ligands turn out to be the perfect additive to slow the liquid droplet evaporation without introducing other impurities. Figure 2 shows a nanocrystal monolayer with remarkable degree of ordering produced by maintaining a long lasting wetting layer. With a dependence on particle concentration, the ordered domain sizes are routinely greater than several microns in size. For the sample in Figure 2, we increased the volume fraction of dodecanethiol to 6.3×10^{-3} . The gold nanocrystal concentration is estimated to be $1.2 \times 10^{13} \text{ mL}^{-1}$. A total of 10 μL of this colloid was deposited onto a 4 mm \times 3 mm Si_3N_4 substrate, which was placed on a stand so that losing any liquid by capillary forces between the tweezers was not a concern. The colloid was allowed to dry undisturbed for 1 h. The excess thiol in the solution slowed the evaporation of toluene and prevented the solvent from dewetting the surface even after an hour. The remaining wetting layer on the surface allowed

nanocrystals to diffuse and self-assemble. After 1 h, this wetting layer then was quickly pumped off the substrate by applying a vacuum.

We found a sharp transition between the ordered monolayer region and the bare substrate region, indicating that lateral diffusion in the wetting-liquid layer is mainly driven by the interaction between particles. We also observed a slight increase of the size distribution near the edge of the monolayer domain, indicating that the size-selective process occurs simultaneously with the assembly process.

For monolayers formed by nanocrystals dissolved in pure toluene, the average interparticle distance is smaller and varies over a wider range, compared with the highly ordered monolayers (Figure 2). Image analysis of Figure 1c gives a distribution of the center-to-center distance between nearest neighbor, with a mean \bar{d} of 7.0 nm and full width at half-height (fwhh) of 2.5 nm. The same analysis in Figure 2 gives that \bar{d} of 7.9 nm with a much narrower fwhh of 1.2 nm.²⁷ Most likely, the reason is that, after repeated washing with ethanol, the amount of thiol molecules attached to the nanocrystal surfaces is relatively small, which allows for ligands to pack with much more flexibility between neighboring particles. By contrast, in the highly ordered superlattices, the higher surface density of thiol molecules constrains the ligands' packing arrangement between particles.

The formation of well-ordered bilayers can be achieved by increasing the nanocrystal concentration while maintaining the concentration of the solvent mixture. Figure 3 shows a typical bilayer formed by depositing 10 μ L of colloid with a particle concentration of approximately 2.4×10^{13} mL⁻¹. The structure of this bilayer is different from the structures reported earlier,^{28–31} in which the second-layer nanocrystals sit on the two-fold saddle sites between the first-layer particles, forming either line or ring structures. These structures were attributed to packing arrangements of nanocrystal facets. In the slightly disordered arrays, we also observed two-fold arrangement. However, in our highly ordered bilayers, the second-layer particles position themselves almost exclusively on the three-fold sites of the monolayer underneath. This indicates that, for the well ligated nanocrystals, nanocrystal facets are completely shielded from the neighboring particles and, therefore, have no influence in determining the packing structure. Much like hard sphere packing, three-fold sites are more favorable.

The presence of excess dodecanethiol in the solvent mixture plays an important role in the formation of highly ordered superlattice structures. First of all, it provides a lasting wetting layer on the silicon nitride surface for nanocrystals to diffuse to their equilibrium sites. Molecular dynamics simulations done by Luedtke and Landman have shown that thiol molecules can lubricate the interface, giving nanocrystals a high surface mobility.³² We found that a critical thiol concentration is needed to maintain a lasting wetting layer on the surface. Below this critical concentration (6.3×10^{-3} in our experiments), partial dewetting occurred after 1 h. In these cases, instead of extended monolayers or bilayers, clusters of multilayers were formed (Figure 4). We believe that these clusters were formed in the dewetting droplets where the nanocrystal concentration increased beyond the single particle-cluster phase transition boundary. Similar cluster formation in a concentrated bulk colloid has been observed by photon correlation spectroscopy.³³ This also indicates that maintaining the particle concentration below the critical concentration in the wetting layer is crucial for the formation of extended monolayers and bilayers. The superlattices formed in the wetting layer are very robust, as is shown by the fact that vacuum drying did not damage the ordering.

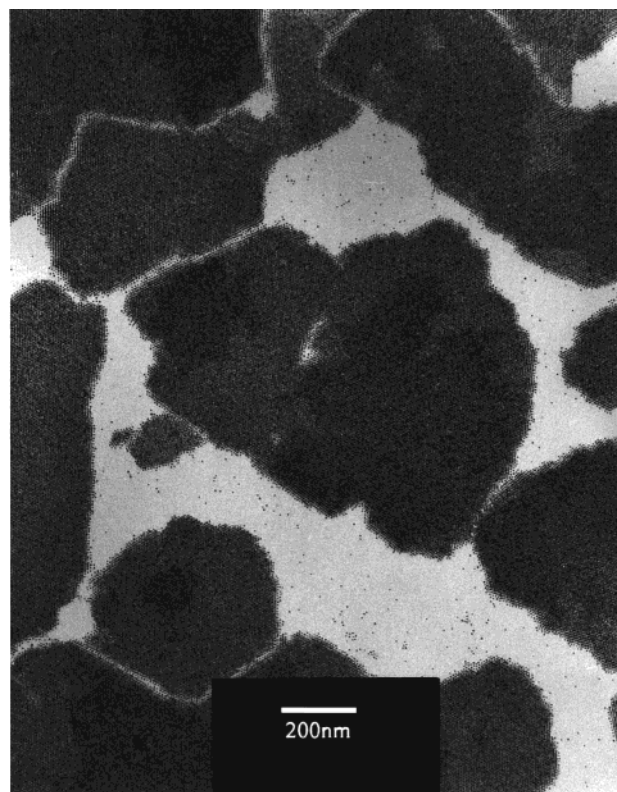


Figure 4. Multilayer clusters formed on the silicon nitride substrate when partial dewetting occurs below the critical thiol concentration. The clusters are highly ordered as well. The bright regions show the bare substrate with a few isolated nanocrystals.

Molecular simulations³² have shown that thiol molecules formed interlocking bundles when nanocrystals form superlattices. High-resolution TEM on silver nanocrystal superlattices supports this idea.³⁴ We believe that the robustness of our extended monolayers and bilayers provides indirect evidence that interlocking bundles of thiol molecules might contribute significantly to the stability of the superlattice structures.

IV. Conclusion

We have demonstrated that very highly ordered nanocrystal superlattices can be achieved if a stable wetting layer of solvent is maintained on the substrate. We achieved this by using a mixture of dodecanethiol and toluene. Our method produces in a very efficient manner both mono- and bilayers by simply changing the nanocrystal concentration. The abundance of the thiol molecules also helps to interlock particles inside the superlattice, therefore, creating a mechanically robust structure. The near-perfect ordering over several microns makes these superlattices suitable for novel electronic or optical applications that depend on long-range periodicity.

Acknowledgment. The authors acknowledge the support of the W.M. Keck foundation through Grant 991705 and the support of National Aeronautics and Space Administration through Grant NAG8-1687. This work was also supported in part by MRSEC Program of the National Science Foundation under Award Number DMR-9808595. We would like to thank N. Mueggenburg for helping us with image analysis. We are also grateful to T. A. Witten and R. Parthasarathy for valuable discussions.

References and Notes

- (1) Ball, P. *The Self-Made Tapestry: Pattern Formation in Nature*; Oxford University Press: New York, 1999.

- (2) Altmann, S. L. *Band Theory of Solids: An Introduction from the Point of View of Symmetry*; Oxford University Press: New York, 1991.
- (3) Pye, L. D.; La Course, W. C.; Stevens, H. J. *The Physics of noncrystalline solids*; Taylor & Francis: Washington, DC, 1992.
- (4) Murray, C. B.; Norris, D. J.; Bawendi, M. G. *J. Am. Chem. Soc.* **1993**, *115*, 8706.
- (5) Brust, M.; Walker, M.; Bethell, D.; Schiffrin, D. J.; Kiely, C. J. *J. Chem. Soc., Chem. Commun.* **1994**, 801.
- (6) Schaaft, T. G.; Knight, G.; Shafigullin, M. N.; Bor, R. F.; Whetten, R. L. *J. Phys. Chem.* **1998**, *102*, 10643.
- (7) Collier, C. P.; Saykally, R. J.; Shiang, J. J.; Henrichs, S. E.; Heath, J. R. *Science* **1997**, *277*, 1978.
- (8) Black, C. T.; Murray, C. B.; Sandstrom, R. L.; Sung, S. *Science* **2000**, *290*, 1131.
- (9) Whetten, R. L.; Khoury, J. T.; Alvarez, M. M.; Murthy, S.; Vezmar, I.; Wang, Z. L.; Stephens, P. W.; Cleveland, C. L.; Luedtke, W. D.; Landman, U. *Adv. Mater.* **1996**, *8*, 428.
- (10) Collier, C. P.; Vossmeier, T.; Heath, J. R. *Annu. Rev. Phys. Chem.* **1998**, *49*, 371.
- (11) Weller, H. *Angew. Chem., Int. Ed. Engl.* **1996**, *35*, 1079.
- (12) Murray, C. B.; Kagan, C. R.; Bawendi, M. G. *Science* **1995**, *270*, 1335.
- (13) Motte, L.; Billoudet, F.; Pileni, M. P. *J. Phys. Chem.* **1995**, *99*, 16425.
- (14) Kiely, C. J.; Fink, J.; Brust, M.; Bethell, D.; Schiffrin, D. J. *Nature* **1998**, *396*, 444.
- (15) Giersig, M.; Mulvaney, P. *Langmuir* **1993**, *9*, 3408.
- (16) Yin, J. S.; Wang, Z. L. *Phys. Rev. Lett.* **1997**, *79*, 2570.
- (17) Motte, L.; Billoudet, F.; Lacaze, E.; Douin, J.; Pileni, M. P. *J. Phys. Chem.* **1997**, *101*, 138.
- (18) Remacle, F.; Collier, C. P.; Markovich, G.; Heath, J. R.; Banin, U.; Levine, R. D. *J. Phys. Chem.* **1998**, *102*, 7727.
- (19) Korgel, B. A.; Fitzmaurice, D. *Phys. Rev. Lett.* **1998**, *80*, 3531.
- (20) Ohara, P. C.; Gelbart, W. M. *Langmuir* **1998**, *14*, 3418.
- (21) Gelbart, W. M.; Sear, R. P.; Heath, J. R.; Chaney, S. *Faraday Discuss.* **1999**, *112*, 299.
- (22) Lin, X. M.; Sorensen, C. M.; Klabunde, K. J. *J. Nanoparticle. Res.* **2000**, *2*, 157.
- (23) Morkved, T. L.; Lopes, W. A.; Hahm, J.; Sibner, S. J.; Jaeger, H. M. *Polymer* **1998**, *39*, 3871.
- (24) Deegan, R. D.; Bakajin, O.; Dupont, T. F.; Huber, G.; Nagel, S. R.; Witten, T. A. *Nature* **1997**, *389*, 827.
- (25) Ge, G.; Brus, L. E. *J. Phys. Chem. B* **2000**, *104*, 9573.
- (26) Widmann, J. F.; Heusmann, C. M.; Davis, E. J. *Colloid Polym. Sci.* **1998**, *276*, 197.
- (27) Both fwhhs were over estimated by the image analysis program because of the difficulty of finding the exact centers of nanocrystals. However, this does not affect the average distance between the nanocrystals nor does this affect the general trend of fwhh comparison.
- (28) Korgel, B. A.; Fullam, S.; Connolly, S.; Fitzmaurice, D. *J. Phys. Chem.* **1998**, *102*, 8379.
- (29) Wang, Z. L. *Adv. Mater.* **1998**, *10*, 13.
- (30) Fink, J.; Kiely, C. J.; Bethell, D.; Schiffrin, D. J. *Chem. Mater.* **1998**, *10*, 922.
- (31) Zanchet, D.; Moreno, M. S.; Ugarte, D. *Phys. Rev. Lett.* **1999**, *82*, 5277.
- (32) Luedtke, W. D.; Landman, U. *J. Phys. Chem.* **1996**, *100*, 13323.
- (33) Lin, X. M.; Wang, G. M.; Sorensen, C. M.; Klabunde, K. J. *J. Phys. Chem.* **1999**, *103*, 5488.
- (34) Wang, Z. L.; Harfenist, S. A.; Whetten, R. L.; Bentley, J.; Evans, N. D. *J. Phys. Chem.* **1998**, *102*, 3068.